Title

Double helical structure of the twist-bend nematic phase investigated by resonant X-ray scattering at the carbon and sulfur K-edges

Journal

Soft Matter, 14(48)

ISSN

1744-683X

Authors

Salamończyk, Mirosław

Mandle, Richard J

Makal, Anna

et al.

Publication Date

2018-12-12

DOI

10.1039/c8sm01215f

Peer reviewed

Journal Name

COMMUNICATION

Double helical structure of the twist-bend nematic phase by resonant x-ray scattering at the carbon and sulfur K-edges

Received 00th January 20xx,
Accepted 00th January 20xx

DOI: 10.1039/x0xx00000x

www.rsc.org/

Mirosław Salamończyk,*[a,b] Richard J. Mandle,[c] Anna Makal,[b] Alexander Liebman-Peláez,[a] Jun Feng,[a] John W. Goodby,[c] Chenhui Zhu*[a]

The mesogenic dimer displaing nematic and N_{TB} phases was investigated by resonant x-ray scattering at both C and S absorption K-edges and supported by the single x-ray crystallography. In the crystal the resonant studies revealed the forbidden reflection in non-resonant diffraction similar to that found in the N_{TB} phase. The lack of a second harmonic in both C and S resonant X-ray scattering supports the double helical structure of the twist-bend nematic phase.

Soft-matter systems, such as polymers or liquid crystals, are multi-tasking materials used in a growing number of applications. These fluid systems can exhibit periodic structures on the scale of a few nanometers to hundreds of nanometers, and as such this requires the development of new techniques for studying their structure *in situ*. There are two main types of molecular ordering in liquid crystals: positional and orientational. The presence of only orientational order is characteristic of the nematic phase. In lamellar and columnar phases both positional and orientational orders of molecules are observed. The degree of orientational order of molecules in liquid crystal phase is typically determined by NMR,[1] EPR[2] or optical methods,[3–5] while the presence and range of the positional order can be readily investigated using x-ray diffraction methods. In general, the molecular orientation can be deduced by analysing the azimuthal distribution of x-ray signals,[6,7] but the results are strongly influenced by the macro alignment of the sample. If the molecular orientation is modulated on the meso scale of nanometers then using mentioned above conventional methods to probe such orientational modulation becomes more problematic. Examples of such phases with meso range - orientational order are helical nanofilament phase (HNF),[8,9] twist grain boundary smectics,[10] blue phases[11] or the recently discovered twist-bend nematic phase, N_{TB}.[12] In 2013 two groups[13,14] independently suggested helical structure of N_{TB} phase despite the fact that the phase is formed by achiral molecules. In this phase, there is lack of positional ordering but the molecules form a very short pitch heliconical structure. The hint regarding the periodic structure of this phase came from freeze fracture transmission electron microscopy (FFTEM); this technique allows the nanoscale structure to be seen in a replica taken from the frozen organic material. However, the main limitation of FFTEM is complicated sample preparation, which does not exclude the possibility of sample crystallization. Another technique to visualize such periodic structure, even more limited, is atomic force microscopy (AFM), which can only probe the sample surface.[15] The unambiguous proof of the helical structure of the N_{TB} phase was obtained by means of soft resonant x-rays (RSoXS).[16] Resonant technic relies on tuning beam energy to the absorption edge of a specific element, which leads to a tensorial scattering form factor of the resonant atoms. One advantage of RSoXS is that virtually all liquid crystal materials can be tested without special chemical modifications, because the soft x-ray energy covers the absorption range of the light elements present in organic materials (C, N, O). The disadvantage of using soft x-ray radiation is that it requires a high vacuum thus making *in situ* measurements challenging. An alternative way to get the same information as with soft x-ray is to use higher energy x-rays, such as tender or hard[17] x-rays which do not required a high vacuum and the experiments are less time consuming. Tender resonance scattering has been successfully applied to determine the helical structure of chiral smectic phases,[18,19]

[a] *Advanced Light Source, Lawrence Berkeley National Laboratory, 1 Cyclotron Rd, Berkeley, CA, 94720, USA*
E-mail: chenhuizhu@lbl.gov
[b] *Faculty of Chemistry, University of Warsaw, Żwirki i Wigury 101, 02-089 Warsaw, Poland*
E-mail: m.salamonczyk@uw.edu.pl
[c] *Department of Chemistry, University of York, Heslington, York, YO10 5DD, UK*
† Electronic Supplementary Information (ESI) available: methods and additional results. See DOI: 10.1039/x0xx00000x

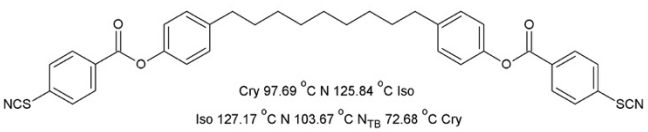

Figure 1 Molecular structure of studied dimer and phase sequences with their temperatures on heating and on cooling taken from differential scanning calorimetry.

giving information about interlayer molecular orientation by revealing peaks forbidden for non-resonant x-ray techniques. This was possible because resonance scattering is sensitive to the local environment of the molecule. Given the wavelength difference (~4.4 nm at C K-edge vs. ~0.5 nm at S K-edge) and practical limitations of instrumental capabilities, RSoXS and TReXS are complementary to each other in accessible q range.

In this communication we combine RSoXS (carbon K-edge) and TReXS (sulfur K-edge) to gain more comprehensive understanding of the twist-bend nematic phase (N_{TB}). The subject of this research is a mesogenic dimer RM1058,[20] incorporating thiocyanate terminal groups (Figure 1), meaning that the element sulfur is only a minority element in the molecular structure at ca. 10 % of total mass. The molecular length (L) of the all trans conformer was estimated to be ~3.6 nm using the Avogadro software. This material shows monotropic twist-bend nematic phase within ~30-degree temperature window and enantiotropic nematic phase above. On cooling the N_{TB} phase material crystalizes at around 72 °C. Such a phase sequence is common for most N_{TB} mesogens, i.e. it is very rare that the other phases (e.g. smectics) appear below the twist-bend nematic.[21–24]

The RSoXS experiment was carried out with energy tuned to the absorption K-edge of carbon. Below 103 °C Bragg diffraction peak appears signifying the N-N_{TB} transition (Figure 2a). The energy scan obtained at 100 °C shows resonant at E_R = 283.6 eV. Near N-N_{TB} transition phase, the scattering peak splits into multiple signals. Such behavior was previously observed for other N_{TB} materials.[16,25,26] In the N_{TB} phase, several degrees below the nematic phase, the single, well

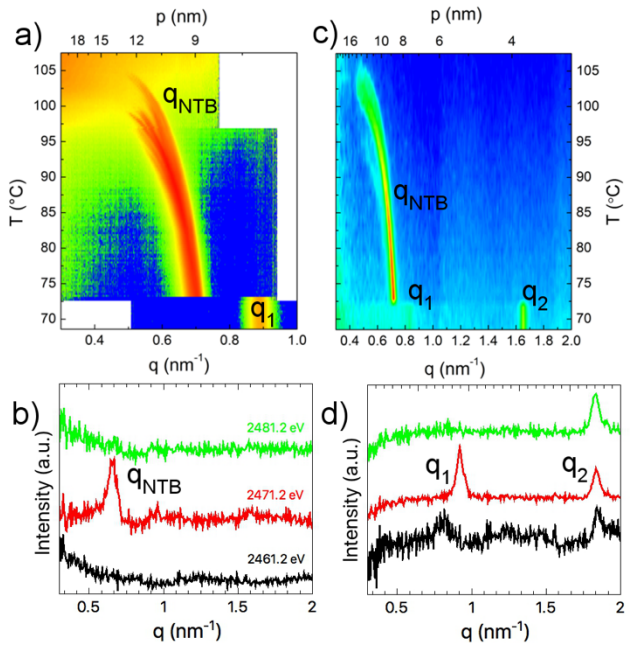

Figure 2 Temperature evolution of wave vector q, measured by RSoXS at C K-edge (283.6 eV), (a) and TReXS at S K-edge (2471.2 eV), (c). Scattering intensity in (a) and (c) is reflected in colours: increases from blue, through green, yellow to red. Intensity vs. wave vector (q) at three different energies (from bottom to top: 2461.2 eV, 2471.2 eV, and 2481.2 eV) registered at 82 °C in the N_{TB} phase (b) and at room temperature in the crystalline phase (d).

developed peak with q_{NTB} = 0.70 nm^{-1} was found, corresponding to a pitch ~9 nm. As temperature lowers, the pitch decreases. In the presently studied material the helical pitch increases on heating from ~9 to ~12.5 nm. Taking into account recent studies on heliconical tilt angle[26,27] and assuming that the molecular length does not change significantly with temperature, each period of the helix consists of ~3-4 molecules per turn. On cooling at ~72 °C the sudden jump of the signal to q_1 = 0.88 nm^{-1} occurs that is associated with the 1st order phase transition, N_{TB}-Cry. It has to be pointed out that different cooling rates or/and different measured spots in the sample may show a weak 1st order phase transition, like seen for the N-N_{TB} phase transition (Figures S6, S7) due to experimental conditions. As expected in the crystal phase the wave vector q_1 is temperature-independent. In both phases the signal is energy dependent and disappears when the energy departs from resonance conditions by +/-10 eV.

The TReXS experiment was carried out with energy tuned around the sulfur absorption K-edge, in the range 2450 – 2490 eV at 82 °C in the N_{TB} (Figure 2b) and at room temperature in the crystal phase (Figure 2d). In both phases resonant appears at E_R = 2471.2 eV, the absorption K-edge of sulfur. In the N_{TB} phase single strong Bragg peak is present at q_{NTB} = 0.70 nm^{-1} which moves to 0.49 nm^{-1} with increasing temperature (Figure 2c), the overall increase of helical pitch in the N_{TB} phase is from ~8.9 to ~12.8 nm and is consistent with pitch length measurements made by RSoXS. Based on theoretical calculations[25] the intensity ratio of $2q_{NTB}/q_{NTB}$ ~ 1 so, the expected $2q_{NTB}$ should be easily detectable at ~1.13 nm^{-1} (at 95 °C). The TReXS experiment shows signal/background intensity ratio > 10, which is sufficient to detect the $2q_0$ peak (Figure 1S). In both resonant X-ray scattering experiments this second harmonic signal is absent in the twist-bend nematic phase, in accordance with the recent studies.[25]

In the crystal phase two Bragg peaks were found at q_1 = 0.82 nm^{-1} and $q_2 = 2q_1$ = 1.65 nm^{-1} both being temperature-independent. The signals show different resonant effect: while q_1 is resonant, q_2 is non-resonant (Figure 2d, 5S) as it is also present at off resonant energy but with somewhat weaker intensity. Periodicity obtained from q_2, d_2 = 3.8 nm, equals to the molecular length L and this means that the crystal is lamellar type and the layers are identical in term of electron density. The resonant q_1 peak corresponds to d_1 = 7.6 nm indicates that the repeated unit is actually equal two molecular lengths. This suggests presence of translational symmetry operations, e.g. a glide plane with the translation vector along the molecular long axis, i.e. a mirror reflection and a translation along the molecular axis. Possible schematic arrangement of molecules in the crystalline phase is shown in Figure 3a.

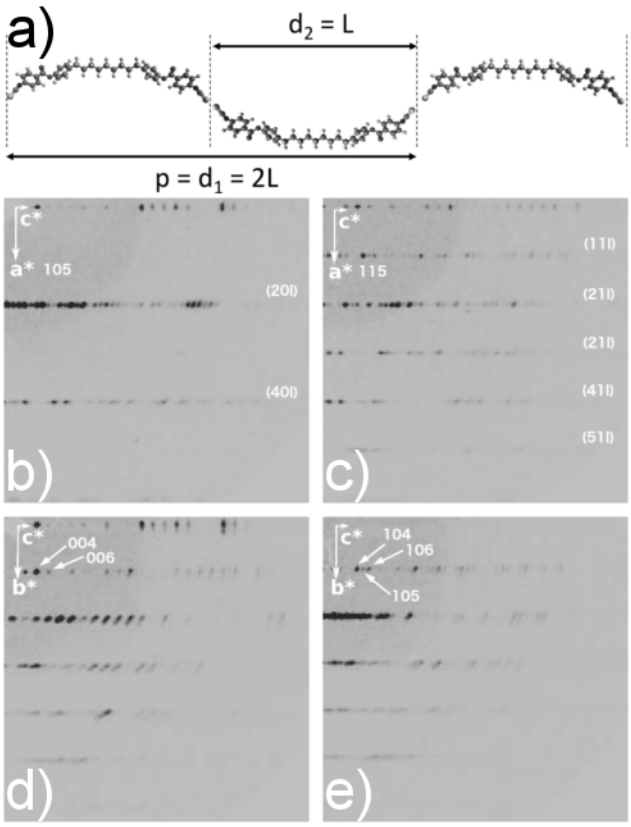

Figure 3 Schematic drawing of molecular packing in layers in the crystal along c direction which is twice the molecular long axis (a). The fragments of experimental reciprocal layers (b) h0l, (c) h1l, (d) 0kl and (e) 1kl, reconstructed from diffraction on a single crystal of studied compound up to resolution of 1.3Å. Indices for selected reflections marked in white. Indices for families of reflections marked in brackets. The reflections with odd h indices are uniformly missing on h0l layer, as compared with h1l, thus fulfilling the h=2n+1 extinction condition for the crystallographic $a_{[100]}$ glide plane. Similarly, reflections with odd l indices are missing from the family of 0kl reflections in the 0kl layer, a contrasted with 1kl layer, fulfilling the l=2n+1 extinction rule for $c_{[100]}$ crystallographic glide plane. The extinction patterns are consistent with $Pca2_1$ crystallographic space group.

As both resonant x-ray experiments reviled resonant and resonantly enhanced Bragg reflections the elastic x-ray diffraction of the crystal phase is needed to fully understand the twist-bend nematic and the crystal phase similarities. The powder x-ray diffraction (PXRD) at room temperature (Figure 9S) as well single crystal x-ray crystallography (Figure 3) were performed to determine actual symmetry of the crystal form of the studied material and consequently to check the character of q_1 and q_2 signals. The resulting space group is most likely $Pca2_1$ in orthorhombic system, with the unit cell parameters a = 0.90536(14) nm, b = 0.94491(17) nm, c = 7.633(2) nm, and the total of eight molecules in crystallographic unit cell (Table 1S). The symmetry operations of $Pca2_1$, namely $c_{[100]}$ and $a_{[010]}$ glide planes, allow only the presence of hkl reflections with even h and l indices in h0l and 0kl reciprocal layers accordingly (Figure 3b,d) while the signals with odd h, l are forbidden and absent in those layers (for comparison see Figure 3c,e with h1l and 1kl layers).

The presence of $c_{[100]}$ glide plane is responsible for the length of the unit cell being twice that of the molecular length. The c-glide plane produces a copy of the first molecule, translated by the length of the molecule (Figure 3).

Based on the data from PXRD and single crystal x-ray diffraction the peak q_2 observed by RSoXS and TReXS can be indexed as 002 and the q_1 peak 001 is forbidden for non-resonant x-ray because it fulfils the l=2n+1 extinction condition (Figure 3S).

Conclusions

In crystal phase in both resonant x-ray experiments the forbidden reflections were revealed. Both soft and tender resonant experiments show that at the transition from N_{TB} phase to crystal the position of the resonant signal changes only slightly. The single crystal x-ray diffraction allowed to index the resonant signal as 001 which is forbidden in non-resonant diffraction due to the presence of $c_{[100]}$ glide plane. Unfortunately, the quality of crystal did not allow determination of the exact distribution of molecules in the crystallographic unit cell. However we can assume that at low temperature range of N_{TB} phase the local structure is similar to the crystal phase and the simple heliconical structure with three molecules per turn is formed with a pitch p = 8.5 nm. While in crystal phase two signals were found by TReXS corresponding to full (double molecular distance) and half pitch (single molecular distance), resonant and non-resonant, respectively, in the twist-bend nematic phase only resonant peak was found (q_{NTB}), corresponding to a full helical pitch. The absence of the second harmonic ($2q_{NTB}$) in the N_{TB} phase shows that the structure has to be either (1) perfectly assembled helices (compare with smectic phases[28]), or (2) unperfect with significantly shifted helices.[25] As known from a numerous elastic x-ray scattering experiments[15,17,29] the N_{TB} phase does not have positional order which automatically rejects option (1). When the helices are shifted by p/4 the $2q_{NTB}$ is cancelled out. This finding suggest that the N_{TB} structure is double-helical with two helices being interlocked and shifted against each other, that agrees with the model recently proposed.[25,30] On heating the helical pitch increases to ~4 molecules per turn with the pitch value ~12.5 nm. The spreading of the resonant signal near N-N_{TB} transition is caused by thermal heterogeneity instead of asymmetric elastic energy as reported previously.[16] The environmental conditions required by the TReXS beamline (*i.e.* a helium atmosphere) allow better temperature control than at RSoXS, where ultra-high vacuum is applied. TReXS experiments show narrow distribution of the heliconical pitch than RSoXS, presumably due to improved temperature homogeneity in the sample.

Summarizing the resonant x-ray techniques of tender and soft energy were shown to be powerful and complementary techniques for investigations of orientational order in soft matter in nanoscale.

Conflicts of interest

There are no conflicts to declare.

Acknowledgements

The authors thank Prof. E. Górecka and Dr. D. Pociecha for discussion and Dr. Cheng Wang for technical support at the 11.0.1.2 beamline at the ALS, LBNL.
M.S. acknowledges the support of the National Science Centre (Poland) under the grant no. 2016/22/A/ST5/00319.
R.M and J.W.G. acknowledge support from the EPSRC under the grant no. EP/M020584/1.
The beamlines 11.0.1.2 and 5.3.1 at the Advanced Light Source at the Lawrence Berkeley National Laboratory are supported by the Director of the Office of Science, Office of Basic Energy Sciences, of the U.S. Department of Energy under Contract No. DE-AC02-05CH11231. This work was supported in part by the National Institute of General Medical Sciences of the National Institutes of Health (NIH) under Award R01GM109019. The content of this manuscript is solely the responsibility of the authors and does not necessarily represent the official views of NIH.

Author contributions

M.S. performed RSoXS, TReXS, and PXRD experiments and analysed the data under direction of C.Z. and J.F; R.M. and J.W.G. synthesized the studied material; A.M. performed single crystal x-ray diffraction and systematic extinction analysis therein; A.L.-P. designed the heating plate at the 5.3.1 beamline at the ALS; M.S., with contributions from all co-authors, wrote the manuscript.

Notes and references

1 R. Y. Dong, in *Annual Reports on NMR Spectroscopy*, ed. G. A. Webb, ELSEVIER ACADEMIC PRESS INC, San Diego, 87th edn., 2016, pp. 41–174.
2 N. Vaupotič, J. Szydlowska, M. Salamończyk, A. Kovarova, J. Svoboda, M. Osipov, D. Pociecha and E. Górecka, *Phys. Rev. E*, 2009, **80**, 030701.
3 W. Kuczyński, B. Żywucki and J. Małecki, *Mol. Cryst. Liq. Cryst.*, 2002, **381**, 1–19.
4 N. Hayashi, A. Kocot, M. J. Linehan, A. Fukuda, J. K. Vij, G. Heppke, J. Naciri, S. Kawada and S. Kondoh, *Phys. Rev. E - Stat. Nonlinear, Soft Matter Phys.*, 2006, **74**, 1–11.
5 Z. Zhang, V. P. Panov, M. Nagaraj, R. J. Mandle, J. W. Goodby, G. R. Luckhurst, J. C. Jones and H. F. Gleeson, *J. Mater. Chem. C*, 2015, **3**, 10007–10016.
6 N. S. Murthy, J. R. Knox and E. T. Samulski, *J. Chem. Phys.*, 1976, **65**, 4835–4839.
7 K. Hongladarom, V. M. Ugaz, D. K. Cinader, W. R. Burghardt, J. P. Quintana, B. S. Hsiao, M. D. Dadmun, W. A. Hamilton and P. D. Butler, *Macromolecules*, 1996, **29**, 5346–5355.
8 L. E. Hough, M. Spannuth, M. Nakata, D. a Coleman, C. D. Jones, G. Dantlgraber, C. Tschierske, J. Watanabe, E. Körblova, D. M. Walba, J. E. Maclennan, M. A. Glaser and N. A. Clark, *Science*, 2009, **325**, 452–456.
9 C. Zhu, C. Wang, A. Young, F. Liu, I. Gunkel, D. Chen, D. Walba, J. Maclennan, N. A. Clark and A. Hexemer, *Nano Lett.*, 2015, **15**, 3420–3424.
10 J. Fernsler, L. Hough, R.-F. Shao, J. E. Maclennan, L. Navailles, M. Brunet, N. V Madhusudana, O. Mondain-Monval, C. Boyer, J. Zasadzinski, J. A. Rego, D. M. Walba and N. A. Clark, *Proc. Natl. Acad. Sci.*, 2005, **102**, 14191–14196.
11 D. C. Wright and N. D. Mermin, *Rev. Mod. Phys.*, 1989, **61**, 385–432.
12 M. Cestari, S. Diez-Berart, D. A. Dunmur, A. Ferrarini, M. R. de la Fuente, D. J. B. Jackson, D. O. Lopez, G. R. Luckhurst, M. A. Perez-Jubindo, R. M. Richardson, J. Salud, B. A. Timimi and H. Zimmermann, *Phys. Rev. E*, 2011, **84**, 031704.
13 V. Borshch, Y.-K. Kim, J. Xiang, M. Gao, A. Jakli, V. P. Panov, J. K. Vij, C. T. Imrie, M. G. Tamba, G. H. Mehl and O. D. Lavrentovich, *Nat. Commun.*, 2013, **4**, 2635.
14 D. Chen, J. H. Porada, J. B. Hooper, A. Klittnick, Y. Shen, M. R. Tuchband, E. Korblova, D. Bedrov, D. M. Walba, M. A. Glaser, J. E. Maclennan and N. A. Clark, *Proc. Natl. Acad. Sci.*, 2013, **110**, 15931–15936.
15 E. Górecka, M. Salamończyk, A. Zep, D. Pociecha, C. Welch, Z. Ahmed and G. H. Mehl, *Liq. Cryst.*, 2015, **42**, 1–7.
16 C. Zhu, M. R. Tuchband, A. Young, M. Shuai, A. Scarbrough, D. M. Walba, J. E. Maclennan, C. Wang, A. Hexemer and N. A. Clark, *Phys. Rev. Lett.*, 2016, **116**, 147803.
17 W. D. Stevenson, Z. Ahmed, X. B. Zeng, C. Welch, G. Ungar and G. H. Mehl, *Phys. Chem. Chem. Phys.*, 2017, **19**, 13449–13454.
18 P. Mach, R. Pindak, A.-M. Levelut, P. Barois, H. Nguyen, C. Huang and L. Furenlid, *Phys. Rev. Lett.*, 1998, **81**, 1015–1018.
19 H. F. Gleeson and L. S. Hirst, *ChemPhysChem*, 2006, **7**, 321–8.
20 R. J. Mandle, E. J. Davis, C.-C. A. Voll, C. T. Archbold, J. W. Goodby and S. J. Cowling, *Liq. Cryst.*, 2015, **42**, 688–703.
21 R. J. Mandle, E. J. Davis, S. a. Lobato, C.-C. a. Vol, S. J. Cowling and J. W. Goodby, *Phys. Chem. Chem. Phys.*, 2014, **16**, 6907.
22 N. Sebastián, M.-G. Tamba, R. Stannarius, M. R. de la Fuente, M. Salamonczyk, G. Cukrov, J. T. Gleeson, S. Sprunt, A. Jakli, C. Welch, Z. Ahmed, G. H. Mehl and A. Eremin, *Phys. Chem. Chem. Phys.*, 2016, 22–24.
23 J. P. Abberley, R. Killah, R. Walker, J. Storey and C. T. Imrie, *Nat. Commun.*, 2018, **228**, 1–7.
24 A. Knezevic, I. Dokli, M. Sapunar, S. Segota, U. Baumeister and A. Lesac, *Beilstein J. Nanotechnol.*, 2018, **9**, 1297–1307.
25 M. Salamończyk, N. Vaupotič, D. Pociecha, C. Wang, C. Zhu and E. Gorecka, *Soft Matter*, 2017, **13**, 6694–6699.
26 M. R. Tuchband, D. A. Paterson, M. Salamończyk, V. A. Norman, A. N. Scarbrought, E. Forsyth, E. Garcia, C. Wang, J. M. D. Storey, D. M. Walba, S. N. Sprunt, C. Zhu, C. T. Imrie and N. A. Clark, *arXiv:1710.00922v2*, 2018.
27 C. Meyer, G. R. Luckhurst and I. Dozov, *J. Mater. Chem. C*, 2015, **3**, 318–328.
28 J. Stamatoff, P. E. Cladis, D. Guillon, T. Bilash and P. Finn, *Phys. Rev. Lett.*, 1980, **44**, 1509–1512.

29 D. A. Paterson, J. Xiang, G. Singh, R. Walker, D. M. Agra-Kooijman, A. Martinez-Felipe, M. Gao, J. M. D. Storey, S. Kumar, O. D. Lavrentovich and C. T. Imrie, *J. Am. Chem. Soc.*, 2016, **138**, 5283–5289.

30 M. R. Tuchband, M. Shuai, K. A. Graber, D. Chen, C. Zhu, L. Radzihovsky, A. Klittnick, L. Foley, A. Scarbrough, J. H. Porada, M. Moran, J. Yelk, E. Korblova, D. M. Walba, A. Hexemer, J. E. Maclennan, A. Matthew and N. A. Clark, *arXiv:1703.10787v1*, 2017.